Supporting Information

Controlling Enzymatic Polymerization from Surfaces with Switchable Bioaffinity

Mohammad Divandari[a,†], Jonas Pollard[b,†], Ella Dehghani,[a]

Nico Bruns[b,§,*], Edmondo M. Benetti[a,§,*]

[a]Laboratory for Surface Science and Technology, Department of Materials, ETH Zürich, Vladimir-Prelog-Weg 5, CH-8093 Zürich, Switzerland

[b]Adolphe Merkle Institute, Chemin des Verdiers 4, CH-1700 Fribourg, Switzerland

† These authors contributed equally

§ These authors contributed equally

* Corresponding authors' email addresses: nico.bruns@unifr.ch, edmondo.benetti@mat.ethz.ch

Characterization of the initiator-functionalized substrates

Table S1. Average static water contact angle of TiO_2 substrates prior and after functionalization with a self-assembled monolayer (SAM) of ATRP initiator, and average dry thickness of the ATRP initiator SAM measured by VASE. The error values for both the contact angle and dry thickness are calculated based on the average and standard deviation of measurements done on 3 different points on the sample.

Water contact angle after cleaning (°)	Water contact angle after functionalization with ATRP initiator (°)	VASE dry thickness of ATRP initiator SAM (nm)
<10 °	61 ± 4°	0.4 ± 0.1

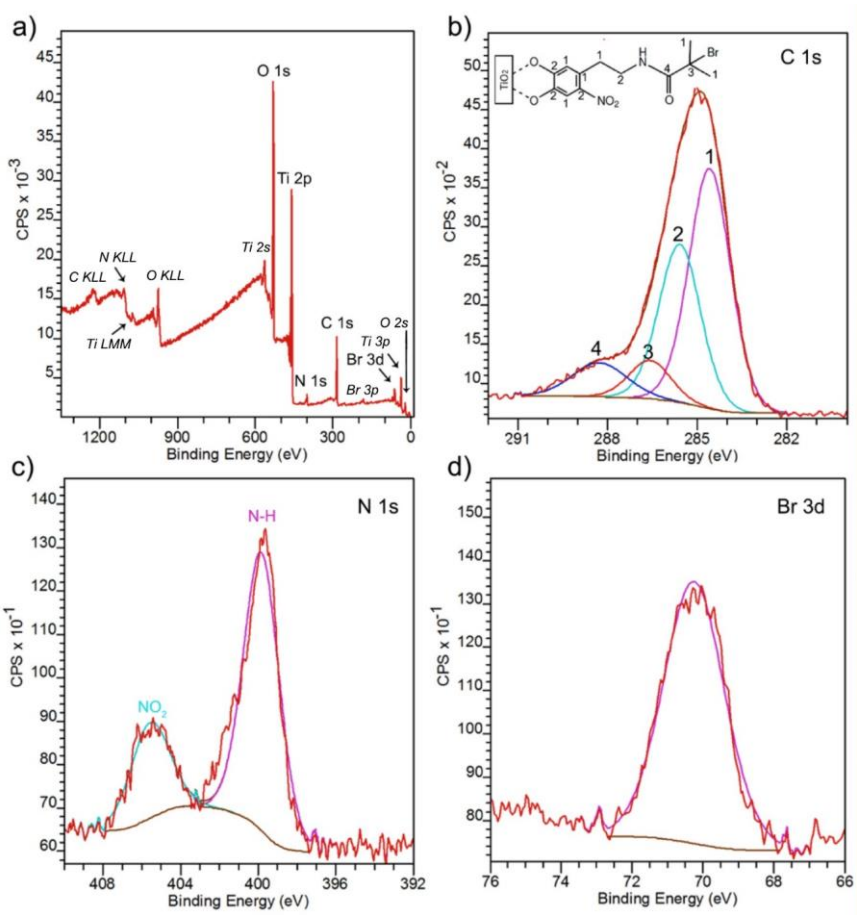

Figure S1. XPS spectra of ATRP initiator SAM on TiO_2 substrates. a) Survey spectra, b) C 1s peak, c) N 1s peak, d) Br 3d peak. The C 1s signal was resolved into four component peaks. The assignments, binding energies, and relative areas of these peaks were consistent with the structure of the ATRP initiator adsorbate. In the N 1s spectra, the ratio of the amine or amide peaks versus the nitro peak is greater than 1, which could suggest a possible reduction of NO_2 to NO_x or some loss of NO_2 during X-ray radiation, as previously reported.[1]

Table S2. Characteristic binding energies for the XPS signals reported in Figure S1.

Element	Binding Energy (ev)
O 1s	528 - 536
Ti 2p	456 - 468
Br 3d	68 - 72
C 1s	282 - 291
N 1s	397 - 408

Additional characterization of the polymer brushes

Table S3. Static water contact angle and dry thickness measured by VASE of PPEGA and PNIPAM brushes synthesized by SI-bioATRP at pH 4 and 25 °C for 480 mins.

	Water Contact angle (°)	VASE dry thickness (nm)
PPEGA	39.5 ± 1.5	11.2 ± 0.7
PNIPAAM	55.0 ± 3.0	7.6 ± 1.5

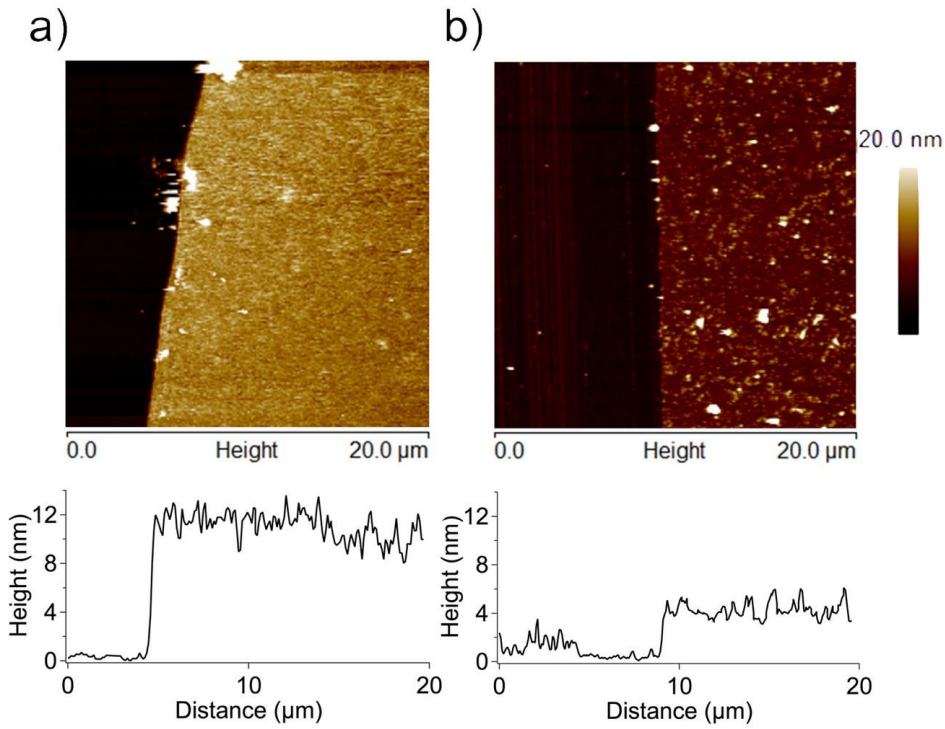

Figure S2. AFM height micrographs of a) PPEGA and b) PNIPAM brushes synthesized by SI-bioATRP at 25 °C and pH 4 for 480 mins. The micrographs were acquired in air. The samples were scratched with a plastic tweezer prior recording in order to estimate the average height of the polymer films. These were 10 ± 3 nm and 5 ± 3 nm for PPEGA and PNIPAM brushes, respectively. The difference between brush thickness measured by VASE and the film height estimated by AFM was due to the compression of the

compliant polymer films by the AFM tip during the measurements, this resulted in an underestimate of the films' thickness.[2]

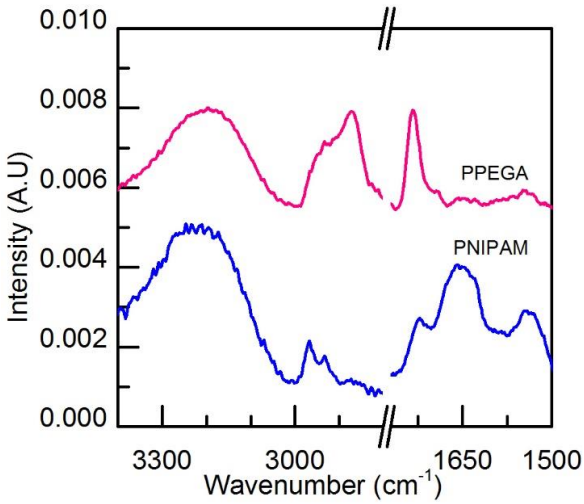

Figure S3. FTIR spectra recorded on PPEGA (pink) and PNIPAM (blue) brushes synthesized at pH 4 and 25 °C after 16 h of polymerization. For PNIPAM, a peak at 1544 cm^{-1} (attributed to N-H secondary amide deformation in the polymer repeating unit) and a strong band at 1658 cm^{-1} (attributed to C=O stretch in secondary amides) confirm the presence and the chemical identity of the polymer film. For PPEGA, the C=O stretching peak centered at 1733 cm^{-1} from the ester group in the repeating unit, and the broad signal from 2800 to 3000 cm^{-1}, related to the C-H stretch, confirm that PPEGA brushes were synthesized on the surface. A broad band included between 3000 to 3400 cm^{-1} was observed for both polymers. This signal was more pronounced for PNIPAM brushes and was attributed to a combination of amide stretching of the polymer and the initiator layer. For PPEGA, this peak was attributed to the amide stretching of the initiator layer.

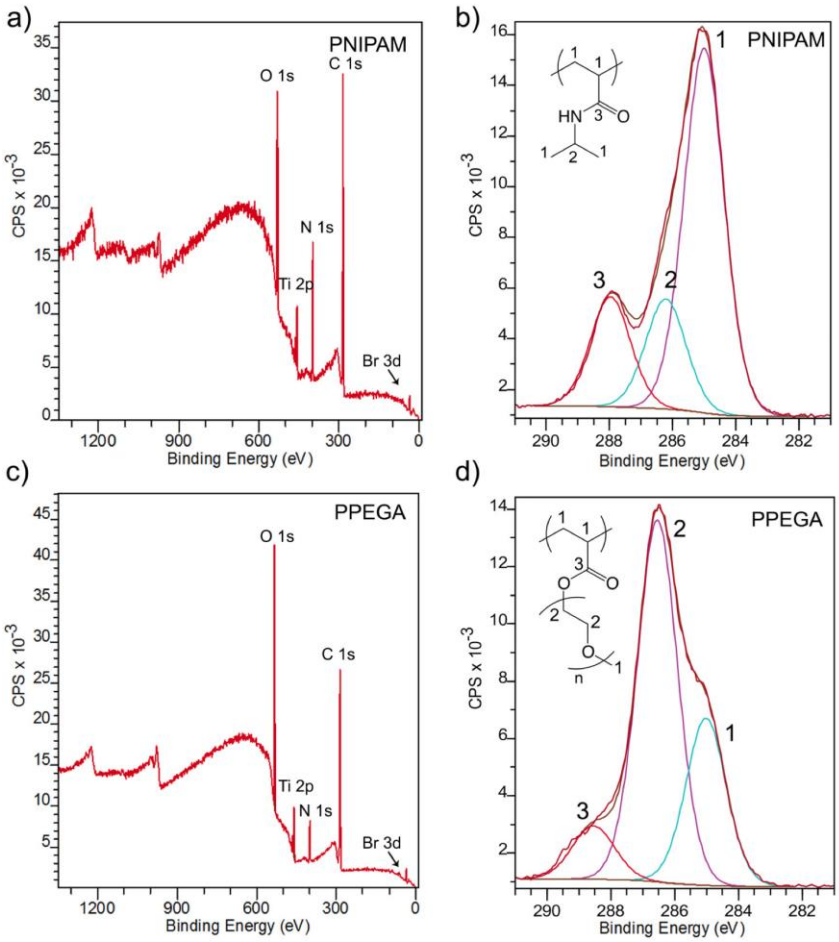

Figure S4. XPS spectra recorded on PNIPAM and PPEGA brushes synthesized by SI-bioATRP at pH 4 and 25 °C with a polymerization time of 16 h. a) Survey XPS spectra from PNIPAM brushes, b) high resolution C 1s peak from PNIPAM, c) survey XPS spectra from PPEGA brushes, d) high resolution C 1s peak from PPEGA. The presence of N 1s peak in the survey spectra of PPEGA was attributed to the underlying ATRP initiator SAM.

Table S4. Relative areas of the component peaks of C 1s from XPS spectra recorded on the different polymer brushes.

	Peak 1 (%)	**Peak 2 (%)**	**Peak 3 (%)**
PNIPAM	61.6	19.2	19.2
PPEGA	61.8	28.9	9.3

XPS analysis of Br-bearing chain ends on PNIPAM brushes synthesized by SI-bioATRP.

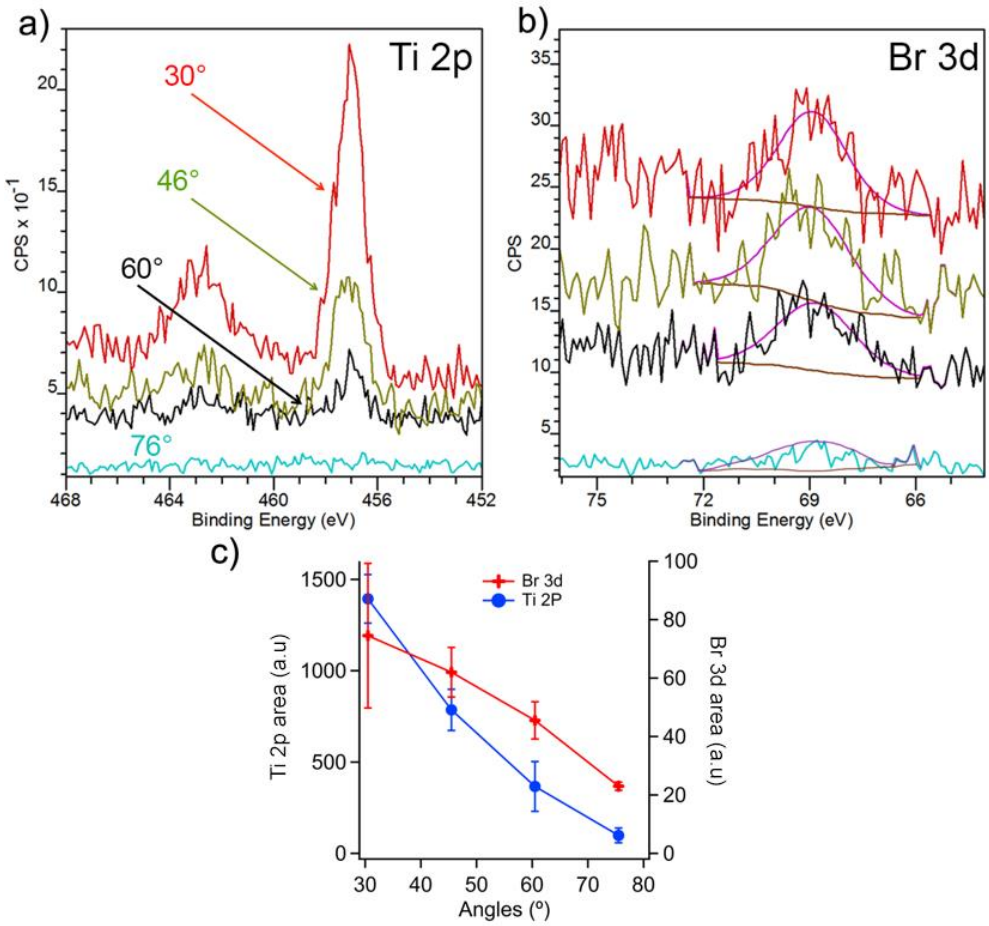

Figure S5. Angle-resolved, high resolution XPS (ARXPS) spectra recorded on PNIPAM brushes of 10 ± 1 nm thickness (measured by VASE) synthesized at pH 4 and 37 ºC after 200 mins of polymerization. The XPS spectra were recorded at four different angles of emission ranging from 76°(corresponding to the signals originating from the outer polymer layer) to 30° (corresponding to the composition of the inner layer). (a) Ti 2p and (b) Br 3d signals from PNIPAM brushes. (c) Peak areas of Br 3d and Ti 2p as a function of emission angle. The signals of Ti and Br decreased from the bulk to the interface of the brush. Since the ARXPS measurements were performed under dry conditions and high vacuum, the polymer chains were in their collapsed morphology with chain ends embedded within the film, thus the presence of Br was mainly recorded within the film (lower angles of emission).

Hb adsorption on to PNIPAM brushes across LCST

QCM-D measurements were carried out to assess the mass of Hb that can adsorb on biocatalytically prepared PNIPAM brushes. To this end, sensors were grafted with a PNIPAM layer, rinsed with cold water to remove all physisorbed proteins, equilibrated in water at 25 °C or 37 °C, and thereafter exposed to an Hb solution at these temperatures. The Hb solution had the same protein concentration as applied during the polymerization, but lacked monomer and a reducing agent. Finally, the surfaces were rinsed with water of the respective temperature. As displayed in Figure S6, Hb did not markedly interact with the swollen

PNIPAM brushes at 25 °C, resulting in an adsorbed protein hydrated mass (Δm_{Hb}) of just 8 ± 2 ng cm^{-2}. In contrast, when the protein adsorption experiment was carried out 37 °C, a clear decrease of Δf after rinsing with 37 °C hot water indicated a more pronounced protein adsorption, with Δm_{Hb} = 27 ± 3 ng cm^{-2}. These QCM results are further supported by the visualization of adsorbed proteins with atomic force microscopy (AFM) at 37 °C but not at 25 °C (Figure S7).

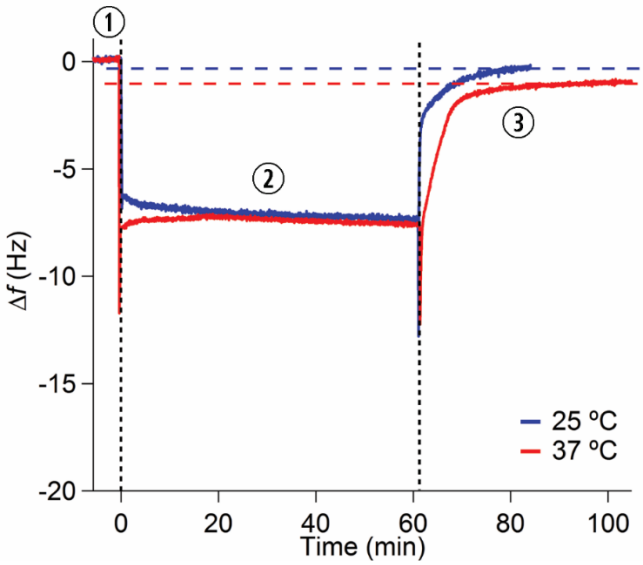

Figure S6. Adsorption of Hb on PNIPAM brushes at 25 °C and 37 °C at pH 4 recorded using QCM-D. A stable baseline (at 27 °C and 37 °C, respectively) was first recorded in ultra-pure water (1), followed by injection of Hb solutions at the two different temperatures (2) and rinsing with ultra-pure water (at 25 °C and 37 °C) (3). The values of Δf between (1) and (3) were translated into a variation of hydrated protein mass (Δm_{Hb}) through fitting with an extended viscoelastic model.[3]

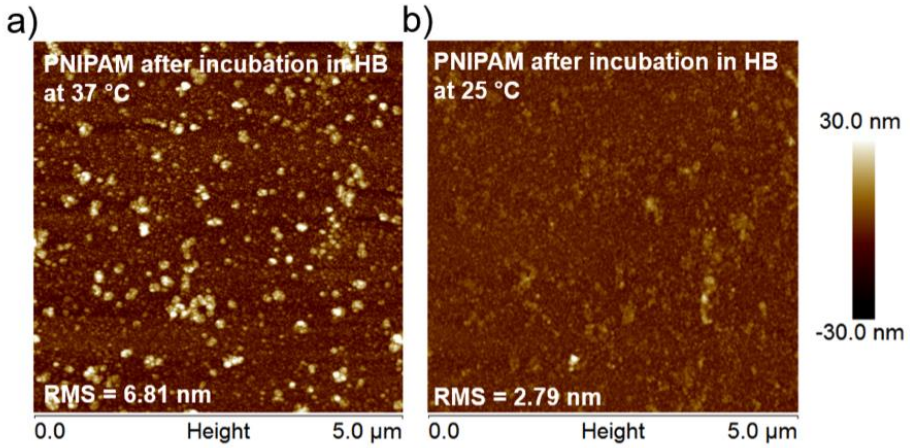

Figure S7. AFM height micrographs measuring the temperature-dependent Hb adsorption on PNIPAM brushes synthesized by SI-bioATRP. The adsorption of Hb at the same concentration used for the polymerizations was imaged at (a) 37 °C and (b) 25 °C. Following incubation in Hb solutions at the two

different temperatures the samples were removed and immediately dried under N_2 without any rinsing. The features the AFM micrographs reported in (a) corresponded to clusters of physisorbed Hb, which were absent in the corresponding micrograph reported in (b). This result confirmed that Hb preferentially adsorbed on PNIPAM brushes at 37 °C (above LCST), but not at 25 °C (below LCST)

SI-bioATRP

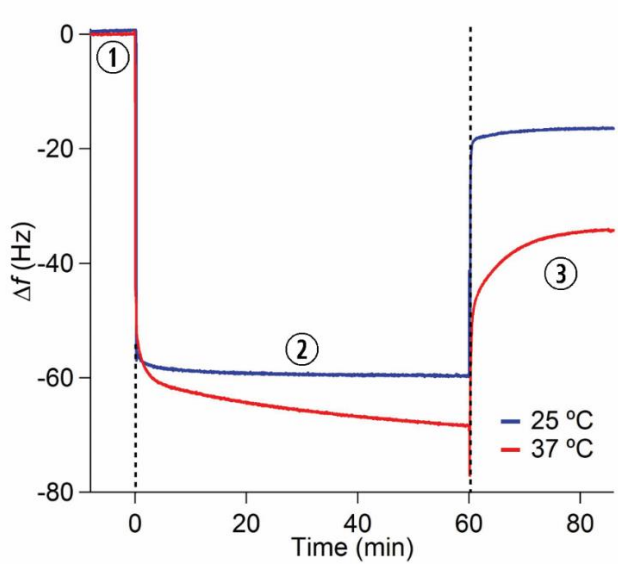

Figure S8. In situ monitoring of SI-bioATRP of NIPAM at 25 °C and 37 °C at pH 4 using QCM-D. Following the collection of a stable baseline in ultra-pure water (1), SI-bioATRP was carried out for 60 min (2). The polymerization was stopped by rinsing the sensor with ultra-pure water, after which a new baseline was recorded (3). The difference in frequency shift (Δf) between the two baselines (1) and (3) correlates to the hydrated mass of the PNIPAM brushes grafted from the sensors, which was quantified according to the extended viscoelastic model.[3] When the polymerization was carried out at 37 °C, a more marked difference in Δf was recorded with respect to the same process carried out at 25 °C, indicating that thicker PNIPAM films have formed 37 °C. It should be remarked that the difference in Δf before and after SI-bioATRP was mostly due to an increase in grafted PNIPAM mass, as the contribution of Hb adsorption was eliminated by rinsing the sensor chips with cold water (water at room temperature) after the polymerization, i.e. during phase (3).

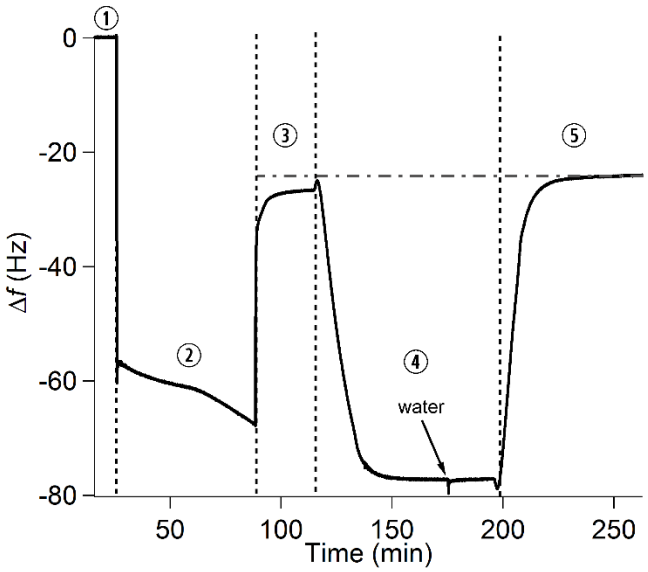

Figure S9. Frequency shifts (Δ*f*) recorded using QCM-D during the SI-bioATRP of NIPAM at pH 4. Following the collection of a stable baseline in ultra-pure water (1), SI-bioATRP was carried out for 60 min at 37 °C (2). The polymerization was stopped by rinsing the sensor with ultra-pure water, after which a new baseline was recorded (3). Later on, the temperature of the QCM-D cell was set to 25 °C and a new baseline was recorded, followed by another washing step (4). Finally the temperature was again raised to 37 °C and maintained until a baseline was reached (5). The difference in Δ*f* between the two baselines (5) and (3) correlates to the desorbed Hb mass.

Effect of additional reducing agent on SI-bioATRP of NIPAM

Figure 1a shows that SI-bioATRP of NIPAM stopped within approx. 200-500 min reaction time. The following experiment was performed to test if the growth of the PNIPAM brushes at 37 °C ended at longer reaction times due to the consumption of the reducing agent NaAsc, PNIPAM brushes were grafted by SI-bioATRP from an ATRP initiator-coated TiO_2 substrate. During this process, aliquots of NaAsc were added to the polymerization solution at intervals of 3 h. The total polymerization time was 9 h. The thickness of the obtained PNIPAM brushes was measured by VASE and compared to the thickness of PNIPAM brushes synthesized by 9 h of SI-bioATRP without adding any additional NaAsc during the reaction. In detail, NIPAM (3.634 mmol), NaAsc (0.0544 mmol, 10.80 mg), Hb (182 nmol, 11.8 mg), and 6.4 ml of 0.1 M acetate buffer (pH 4) were mixed and deoxygenated by nitrogen bubbling for 30 min. Subsequently, the solution was distributed evenly between two flasks containing ATRP initiator-functionalized TiO_2 substrates kept under nitrogen at 37 °C. After 3 and 6 hours, 0.1 ml aliquots of a deoxygenated 108 mg ml^{-1} solution of NaAsc in pH 4 acetate buffer was added to one of the flasks (test sample). After 9 hours of polymerization, the wafers were taken out of the flasks and washed extensively with ultra-pure water. The thickness of the formed PNIPAM brushes was measured with VASE, resulting in 10.5 ± 1.5 nm for the test sample and 9.5 ± 1.0 nm on the control sample (no addition of NaAsc). Since the difference in brush thickness between the two PNIPAM films was not significant, the consumption of NaAsc can be ruled out as the reason for the end of growth of the PNIPAM films at 37 °C at longer reaction times.

Effect of pH on SI-bioATRP of NIPAM

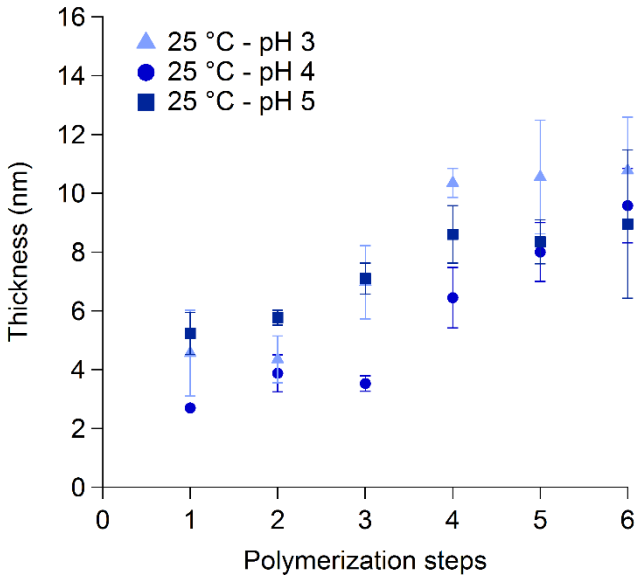

Figure S10. PNIPAM brush thickening during multistep SI-bioATRP at 25 °C performed at different pH values, as measured *ex situ* using VASE. The average and error values (standard deviation) are calculated from n = 9 data points over three samples, with three thickness measurement points on each.

Influence of pH on the structure of Hb at 25 °C and 37°C

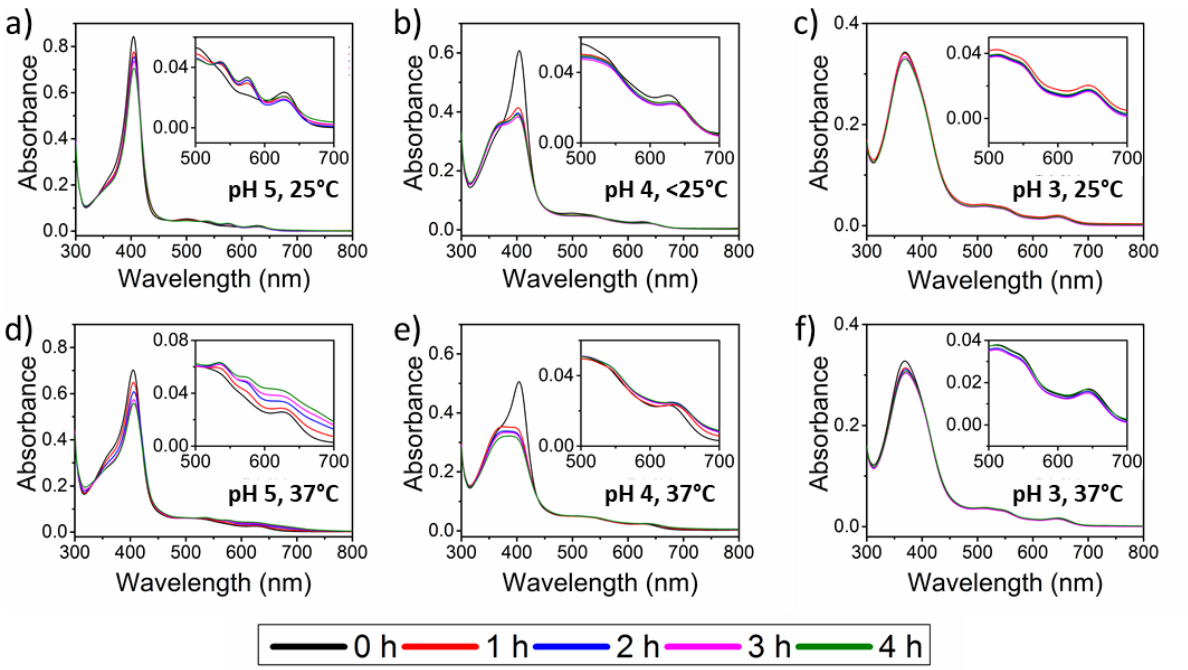

Figure S11. Influence of pH on time-dependent UV-vis spectra of Hb in the presence of NIPAM and NaAsc at polymerization concentrations. a) pH 5/25 °C, b) pH 4/25 °C, c) pH 3/25 °C, d) pH 5/37 °C, e) pH 4/37 °C, f) pH 3/37 °C. The reagent solutions were not deoxygenated prior to the measurements. Please note: The spectra shown in Figure 4b of the manuscript are also reported here as "1 h" in panels d, e and f.

At pH 5 and T = 25 °C, the spectrum indicates that Hb maintained its native conformation and the heme groups of the β-subunits were reduced to Fe(II), while the heme groups of the α-subunits remained in their Fe(III) state (Figure S11a).[62] Hb showed this spectrum for at least 4 h of incubation. At pH 4 and T = 25 °C, the intensity of the Soret band at 406 nm decreased upon exposure of the protein to monomer and reducing agent. This was accompanied by the appearance of an additional band centered at 368 nm (Figure S11b). This transition reached an equilibrium within 1 h of incubation. The coexistence of these two bands suggests the presence of two different Hb species. The peak at 406 nm is indicative of the native form of Hb, while the new band at 368 nm corresponds to the partially unfolded protein, presumably in a molten globular state. This transition became more pronounced when the pH of the polymerization mixture was lowered to 3 (Figure S11c). Under these conditions, the rate of the structural change in the protein is faster than the time that is required to record the UV–vis spectra at the t = 0 h time point. The spectrum, which is stable for at least 4 h, mainly shows the peak related to the acidic conformation of Hb at 368 nm, and only a weak shoulder at 406 nm. Thus, most Hb was present in the partially unfolded molten globule structure. At 37 °C, the UV–vis spectrum of Hb at pH 5 changed to the one of oxygenated intermediate Hb within the first hour of incubation, just as at 25 °C (Figure S11d). The UV–vis spectra recorded at 37 °C at pH 4 and pH 3 were similar to the corresponding spectra collected at 25 °C (Figure S11e, f). Only the equilibrium between the native and acidic conformations of Hb at pH 4 was slightly shifted toward the molten globule state.

Influence of polymerization reagents on the structure of Hb at pH 4

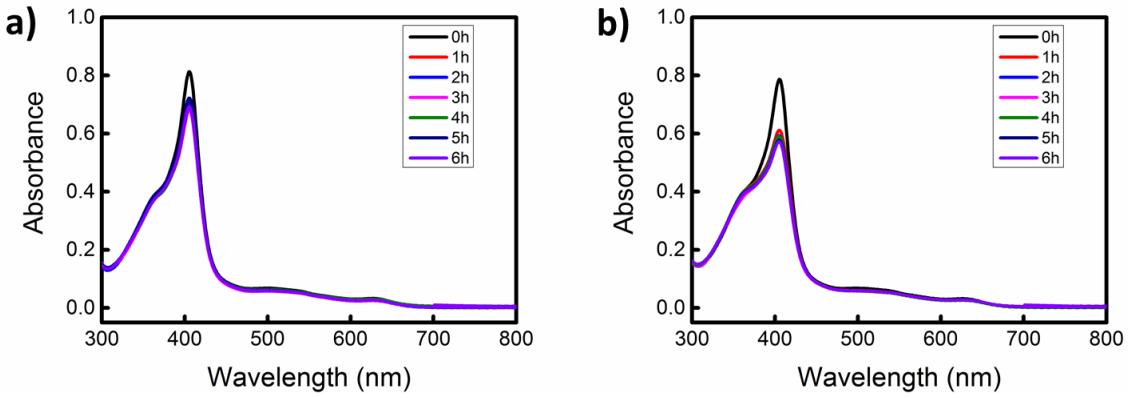

Figure S12. Time-dependent UV-vis spectra of Hb without addition of any reagents at pH 4 and 25 °C (a) and 37 °C (b). Please note: The native spectrum shown in Figure 4b of the manuscript is also reported here.

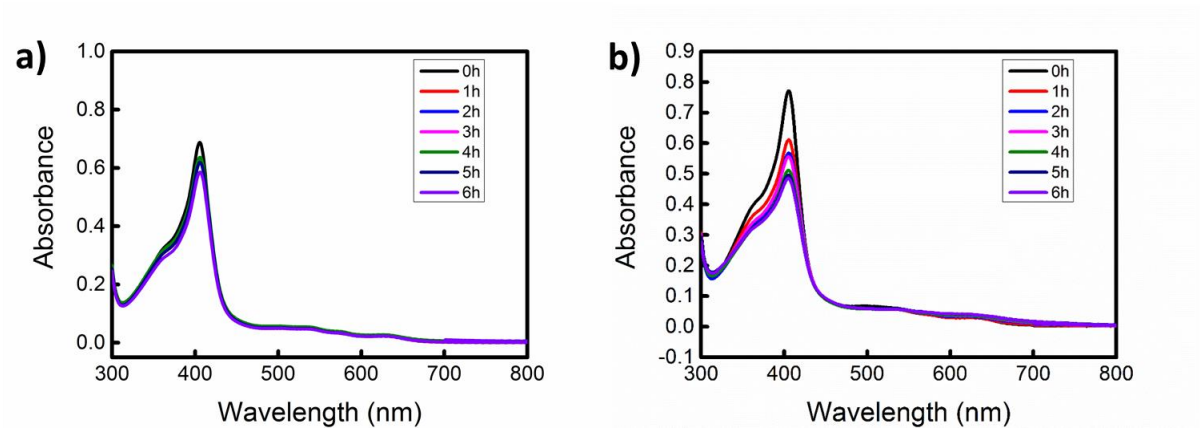

Figure S13. Time-dependent UV-vis spectra of Hb in the presence of 8.5 mM NaAsc at pH 4 and 25 °C (a) and 37 °C (b).

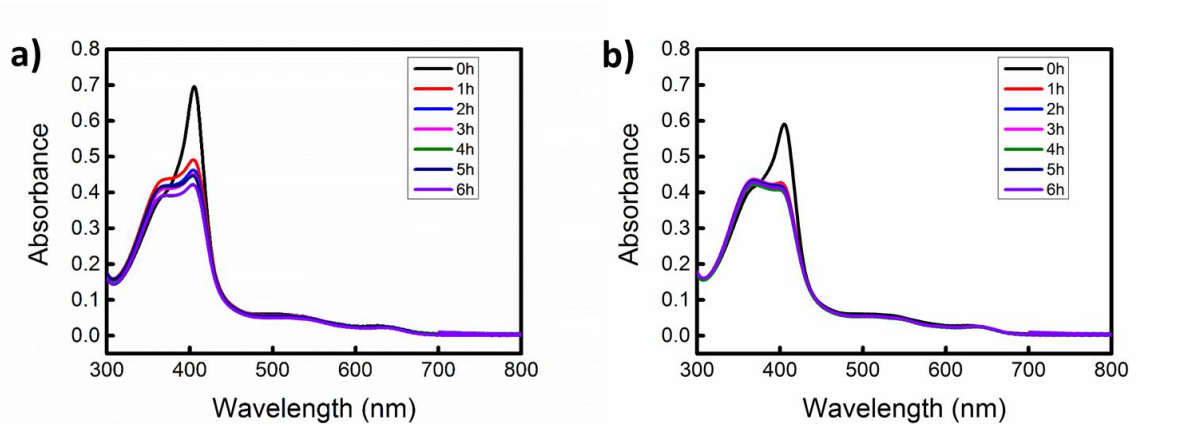

Figure S14. Time-dependent UV-vis spectra of Hb in the presence of 567.8 mM NIPAM at pH 4 and 25 °C (a) and 37 °C (b).

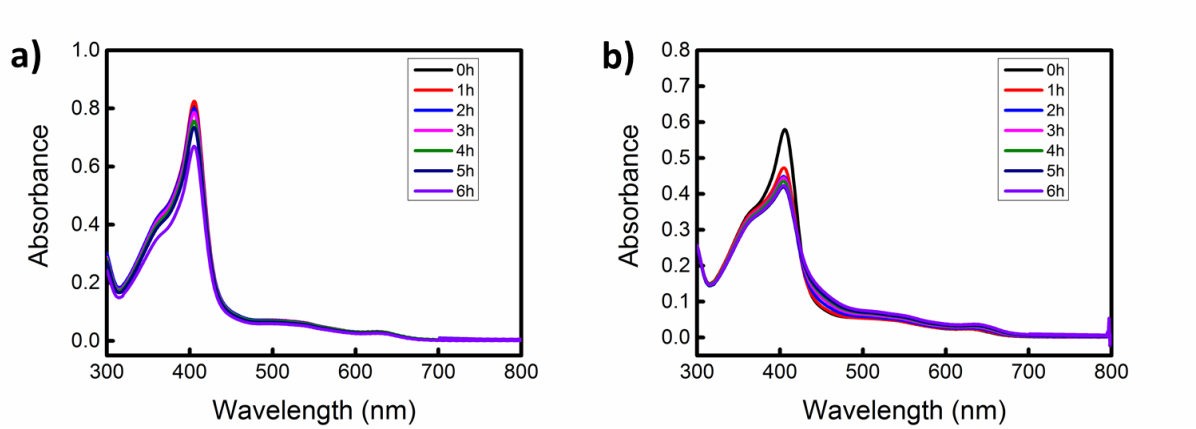

Figure S15. Time-dependent UV-vis spectra of Hb in the presence of 567.8 mM PEGA at pH 4 and 25 °C (a) and 37 °C (b).

Effect of pH on secondary structure of Hb

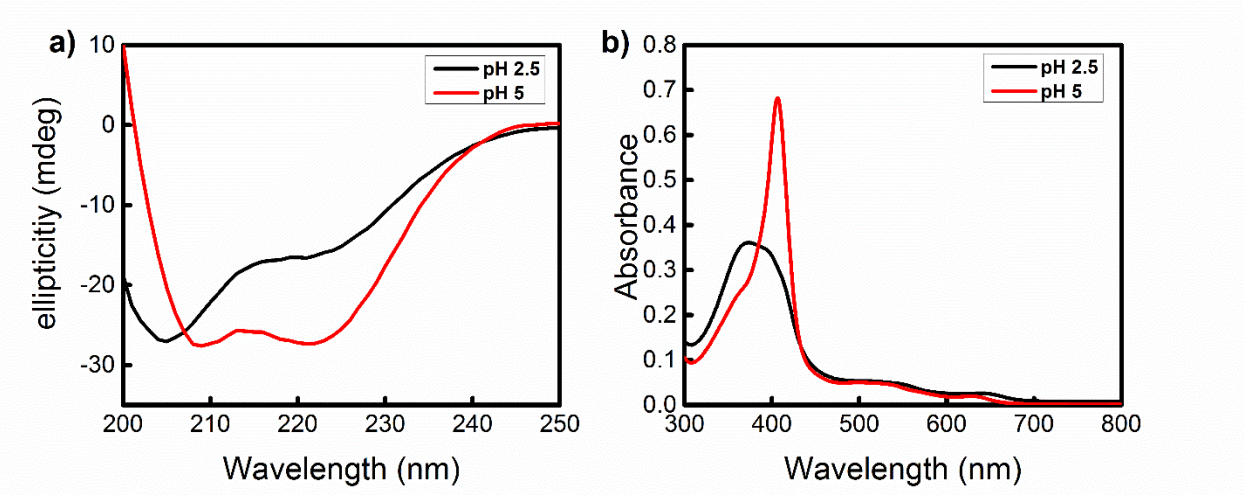

Figure S16. a) Circular dichroism (CD) spectra of Hb at pH 2.5 and pH 5 at room temperature. b) Corresponding UV-vis spectra.

References

1. Rodenstein, M.; Zurcher, S.; Tosatti, S. G. P.; Spencer, N. D., Fabricating Chemical Gradients on Oxide Surfaces by Means of Fluorinated, Catechol-Based, Self-Assembled Monolayers. *Langmuir* **2010,** *26* (21), 16211-16220.
2. Tu, H.; Heitzman, C. E.; Braun, P. V., Patterned poly(N-isopropylacrylamide) brushes on silica surfaces by microcontact printing followed by surface-initiated polymerization. *Langmuir* **2004,** *20* (19), 8313-8320.
3. Hook, F.; Kasemo, B.; Nylander, T.; Fant, C.; Sott, K.; Elwing, H. Variations in coupled water, viscoelastic properties, and film thickness of a Mefp-1 protein film during adsorption and cross-linking: A quartz crystal microbalance with dissipation monitoring, ellipsometry, and surface plasmon resonance study. *Anal. Chem.* **2001**, *73*, 5796-5804.